Supporting Information

An Antimonene/Cp*Rh(phen)Cl/Black Phosphorus Hybrid Nanosheets-based Z-Scheme Artificial Photosynthesis for Enhanced Photo/bio-catalytic CO_2 Reduction

Xiaoyuan Ji[a,c], Yong Kang[b], Taojian Fan[d], Qingqing Xiong[c], Songping Zhang[b,*], Wei Tao[c,*], Han Zhang[d,*]

[a] School of Pharmaceutical Sciences (Shenzhen), Sun Yat-sen University, Guangzhou 510275, China

[b] State Key Laboratory of Biochemical Engineering, Institute of Process Engineering, Chinese Academy of Sciences, Beijing 100190, China, E-mail: spzhang@ipe.ac.cn

[c] Center for Nanomedicine, Brigham and Women's Hospital, Harvard Medical School, Boston, MA 02115, USA, E-mail: wtao@bwh.harvard.edu

[d] Shenzhen Engineering Laboratory of Phosphorene and Optoelectronics, SZU-NUS Collaborative Innovation Center for Optoelectronic Science and Technology, and Key Laboratory of Optoelectronic Devices and Systems of Ministry of Education and Guangdong Province, Shenzhen University, Shenzhen 518060, China, E-mail: hzhang@szu.edu.cn

Experimental Section

1. Materials.

The bulk balck phosphorus (BP) was purchased from Smart-Elements (a commercial supplier). Antimony powder, reduced and oxidized nicotinamide adenine dinucleotide ($NADH/NAD^+$, 98 wt%), formate dehydrogenase from Candida boidinii (FateDH, EC.1.2.1.2), polyethyleneimine (PEI), 2-bromo-1,10-phenthroline (BPT), C18-PEG5000-EO, formic acid, N,N-dimethylformamide (DMF), sodium iodide (NaI), potassium carbonate (K_2CO_3), triethanolamine (TEOA), N-Methyl pyrrolidone (NMP) were purchased from Sigma-Aldrich (St. Louis, MO. USA). Dichloro (pentamethylcyclopentadienyl) rhodium (III) dimer, $[Cp^*RhCl_2]_2$ was purchased from Alfa Aesar. C18-PEG5000-EO was purchased from Shang Hai Ponsure Biotech, Inc.

2. Synthesis of Antimonene Nanosheets (AM NSs).

AM NSs were prepared by a modified liquid-phase exfoliation method with probe sonication in ethanol based on a reported method[1]. Firstly, the commercial antimony powder with an initial concentration of 20 mg/mL was dispersed in ethanol. The solution was sonicated for 8 h in ice-bath at 500 W and centrifuged at 3,000 rpm for 10 min to discard the un-exfoliated bulk antimony. Finally, the suspensions were centrifuged at 10,000 rpm for 30 min and the precipitates were collected for future use.

3. Synthesis of BP NSs.

The BP NSs were prepared by a modified liquid exfoliation of corresponding bulk BP sample[2]. Briefly, 25 mg of the obtained BP was added to 50 mL of NMP. The mixture solution was then sonicated in ice water with a sonic tip for 12 h at 500 W. The resulting brown dispersion was centrifuged at 1000 rpm for 10 min to get rid of unexfoliated bulk BP and the supernatant containing BP NSs was carefully collected. Finally, the suspensions were centrifuged at 10,000 rpm for 30 min and the precipitates were collected for future use.

4. Synthesis of PEI-PEG-C18-M.

Briefly, C18-PEG5000-EO (200 mg) and PEI (10 times of moles of C18-PEG5000-EO) were dissolved in DMF (20 mL) respectively. PEI solution was added into C18-PEG5000-EO solution dropwise. The mixture was allowed to react for 12 h at 60 ^{o}C to form PEI-PEG-C18. A dialysis tube with molecular weight cut-off (MWCO) of 15000 Da was used to remove residue substrates by dialyzing against DMF for 24 h.

For electron mediator binding polymer, BPT was dissolved in DMF (20 mL), and then NaI (1/5 times of moles of BPT) and K_2CO_3 (2 times of moles of BPT) were added to this solution. The mixture was added to PEI-PEG-C18 solution and stirred for 48 h at 60 ^{o}C. A dialysis tube with molecular weight cut-off (MWCO) of 15000 Da was used to remove catalysts and other residue substrates by dialyzing against DMF for 24 h. $[Cp^*RhCl_2]_2$ (2 times of moles of BPT) was added to the solution and stirred for another 1 h. The resulted solution was dialyzed against methanol using membranes with molecular weight cut-off (MWCO) of 1500 Da for 24 h to remove residue substrates.

5. Characterization.

The morphology of the NSs was characterized using transmission electron microscopy (TEM, JEM-2100UHR, JEOL, Japan). The thickness of the NSs was characterized by atomic-force microscopy (AFM, FASTSCANBIO, Germany). The size and surface charge (zeta potential) of the NSs were determined using Dynamic Light Scattering or DLS (15-mW laser, an incident beam of 676 nm; Brookhaven Instruments Corporation). The chemical compositions of the NSs were analyzed by X-ray photoelectron spectroscopy (XPS, ESCALAB 250Xi, Japan) and Fourier transform infrared spectrophotometry (FTIR, Nexus 470, Nicolet, Madison, WI, USA). Elemental mapping was applied to investigate the elementary composition of NSs using an energy-dispersive X-ray spectroscope (EDS) (Inca X-MAX, Oxford, UK), which was directly connected to a scanning electron microscope (JSM-7001F). UV-Vis-NIR spectra of NSs were obtained on an Infinite M200 PRO spectrophotometer. The chemical structures of the NSs were analyzed by X-ray diffraction (XRD) patterns recorded on a Bruker D8

multipurpose XRD system and Raman spectrum was obtained by Aramis made by HORIBA JOBIN YVON. Spectrofluorometric experiments were performed by using RF-5301PC (Shimadzu Co., Japan) with an excitation wavelength of 350 nm. For photocurrent-time (I-T) profiles of AM/M/BP HNSs, the fabrication of the working electrode and other parameters were referred to our previous reports[3].

6. Photo-conversion of Methanol from CO_2.

A quartz reactor equipped with a 450 W Xenon lamp was used to process conversion of methanol from CO_2. Generally, 10 mL buffer solution (100 mM Phosphate, pH 7.0) was bubbled with CO_2 gas for 0.5 h, and then a definite amount of each component involved in the artificial photosynthesis systems was added to reach a final concentration of 15w/v% TEOA, 0.2 mg/mL AM NSs or BP NSs, 0.1 mM M, 0.3 units/mL FateDH, FaldDH, and ADH and 0.1 mM NAD^+. The reaction was carried out under constant pressure at 0.3 MPa. At time intervals, 20 μL of the sample was taken from the reaction mixture for methanol concentration measurement after pressure release. The conversion of CO_2 to methanol using AM/M/BP NSs was also performed under the same conditions as above. A methanol concentration was detected by gas chromatography (Agilent 7890A) equipped with a flame ionization detector (FID) and an Agilent HP-FFAP gas column (25m×0.320mm×0.50μm) [3b, 3c].

7. Detection and calculation of quantum efficiency.

To determine the quantum efficiency (QE) of developed AM/M/BP HNSs for photocatalytic NADH regeneration, the reaction conditions were as same as photocatalyzing NADH regeneration, and the number of incident photons was measured using a silicon photodiode with integrating sphere, and the quantum efficiency was calculated using the equation below:

Quantum efficiency (%) = 2 ß (Moles of NADH produced/Moles of incident photons) ß 100

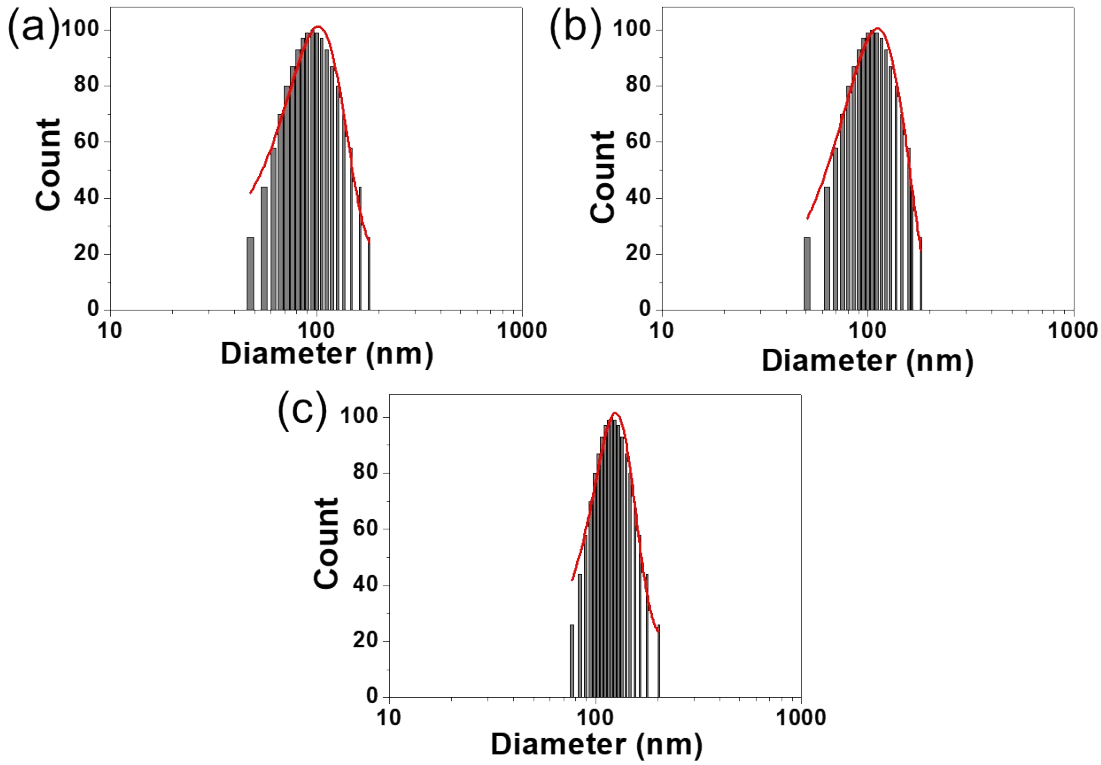

Figure S1. The size distribution of AM, BP, and AM/M/BP HNSs.

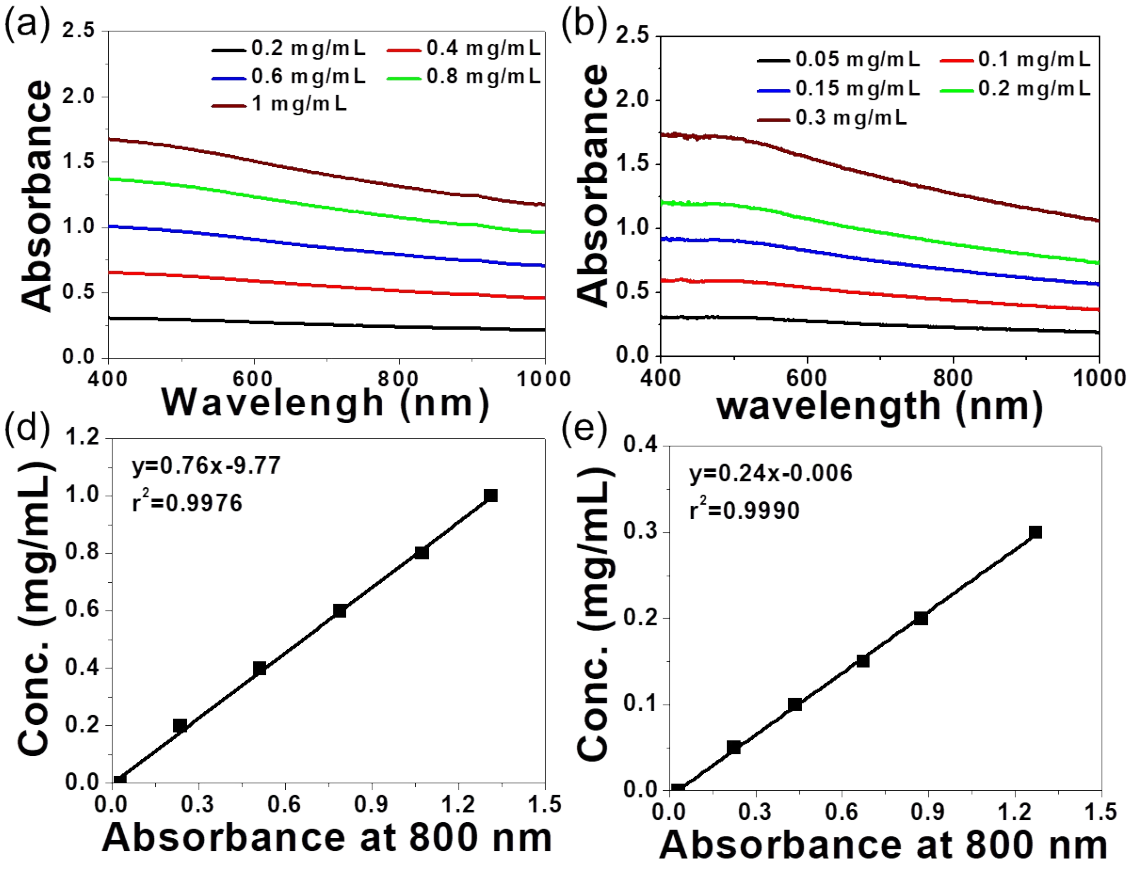

Figure S2. Absorbance spectra of (a) AM and (b) BP NSs dispersed in water at different concentrations. Normalized absorbance intensity of (c) AM and (d) BP NSs divided by the characteristic length of the cell (A/L) at different concentrations for λ=800 nm.

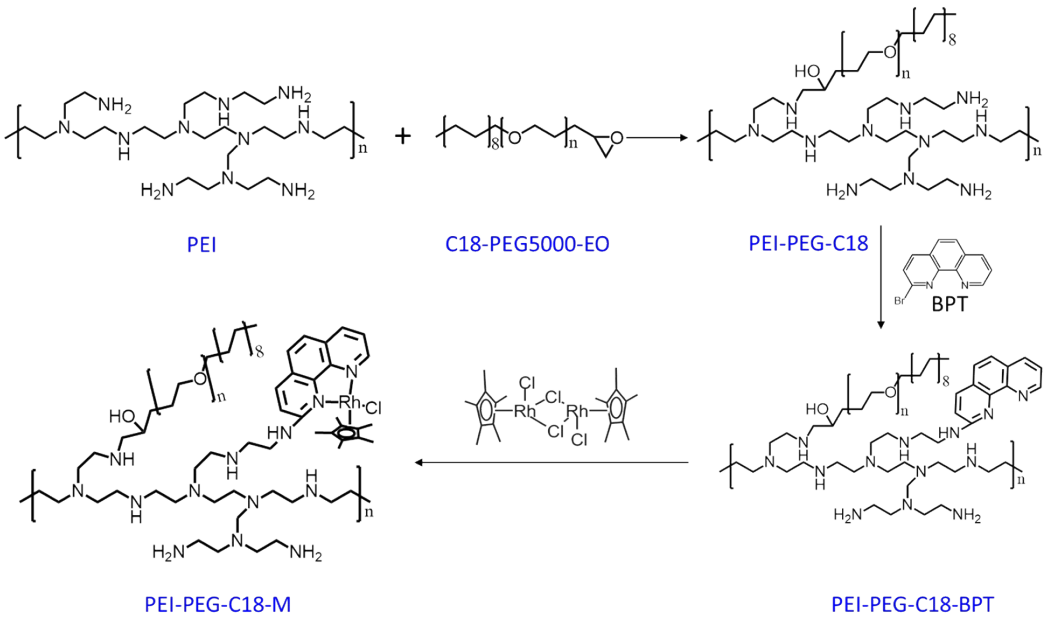

Figure S3. Synthesis route of PEI-PEG-C18-M.

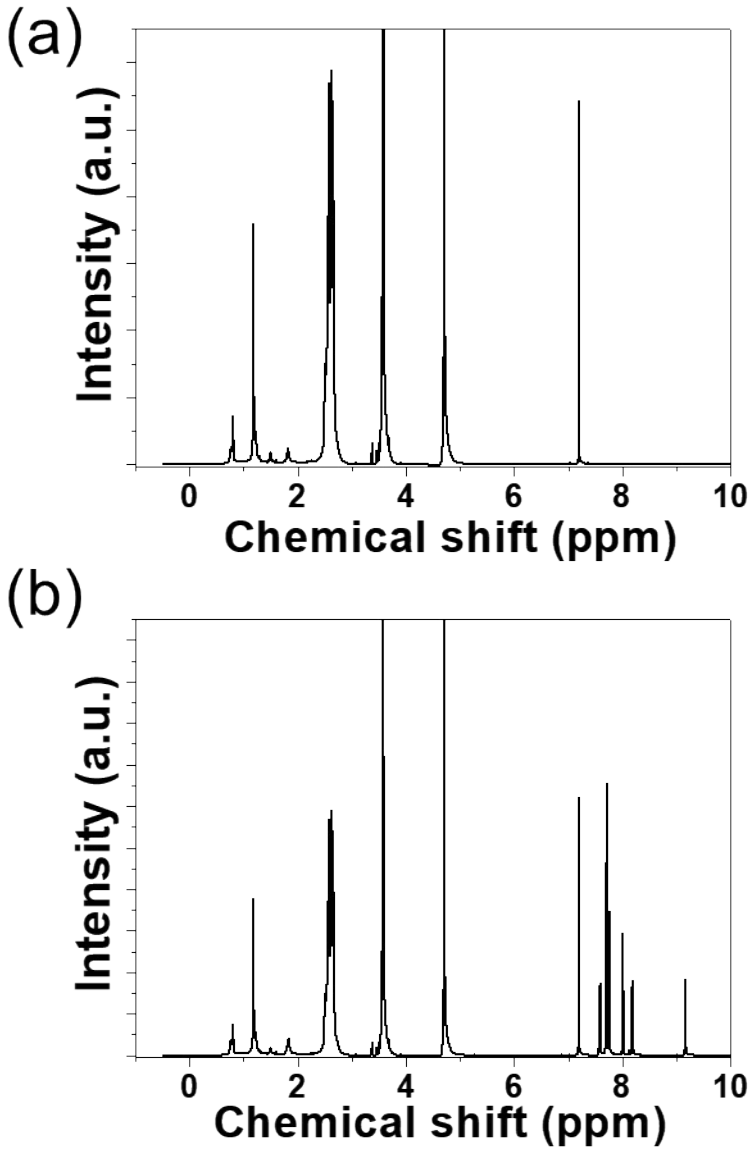

Figure S4. [1]HNMR spectra of (a) PEI-PEG-C18 and (b) PEI-PEG-C18-M.

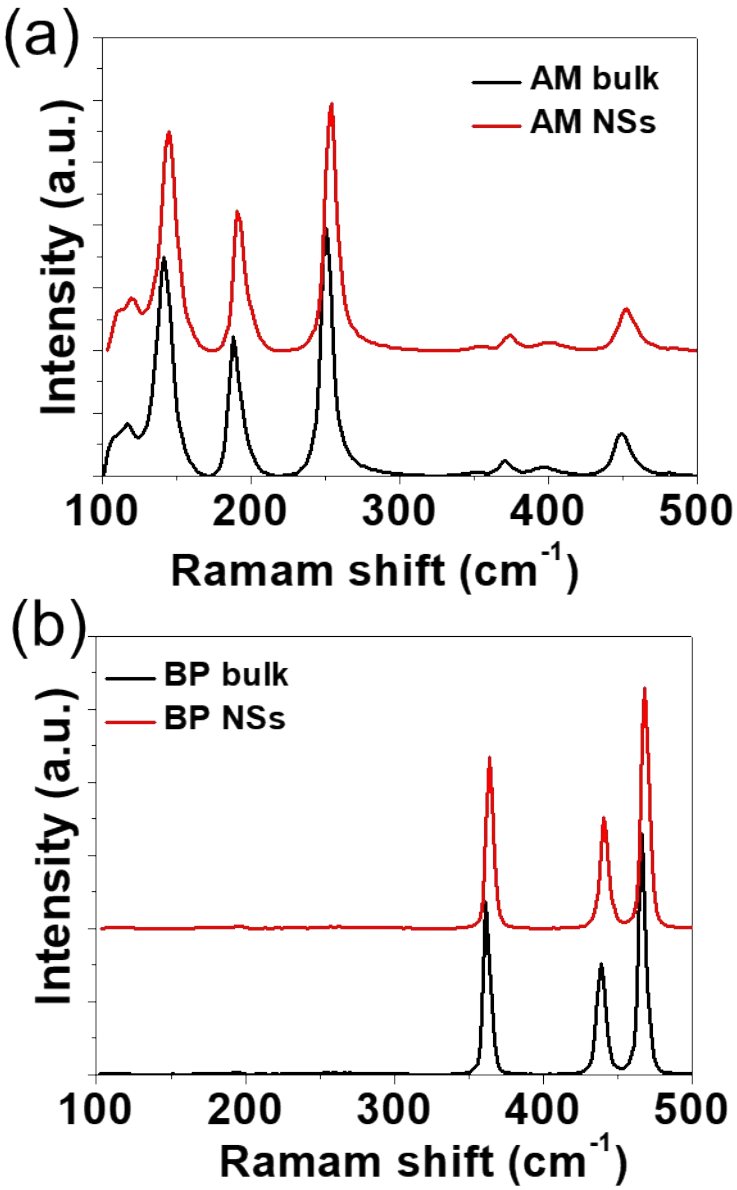

Figure S5. Raman spectra of (a) AM bulk and prepared AM NSs and (b) BP bulk and prepared BP NSs.

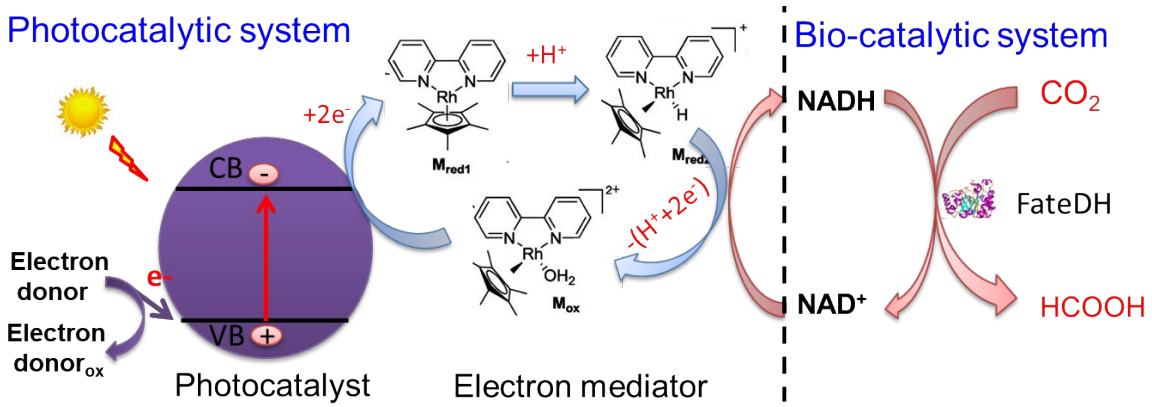

Figure S6. Schematic illustration of the AM/M/BP HNSs based APS for carrying out CO_2 conversion to formic acid.

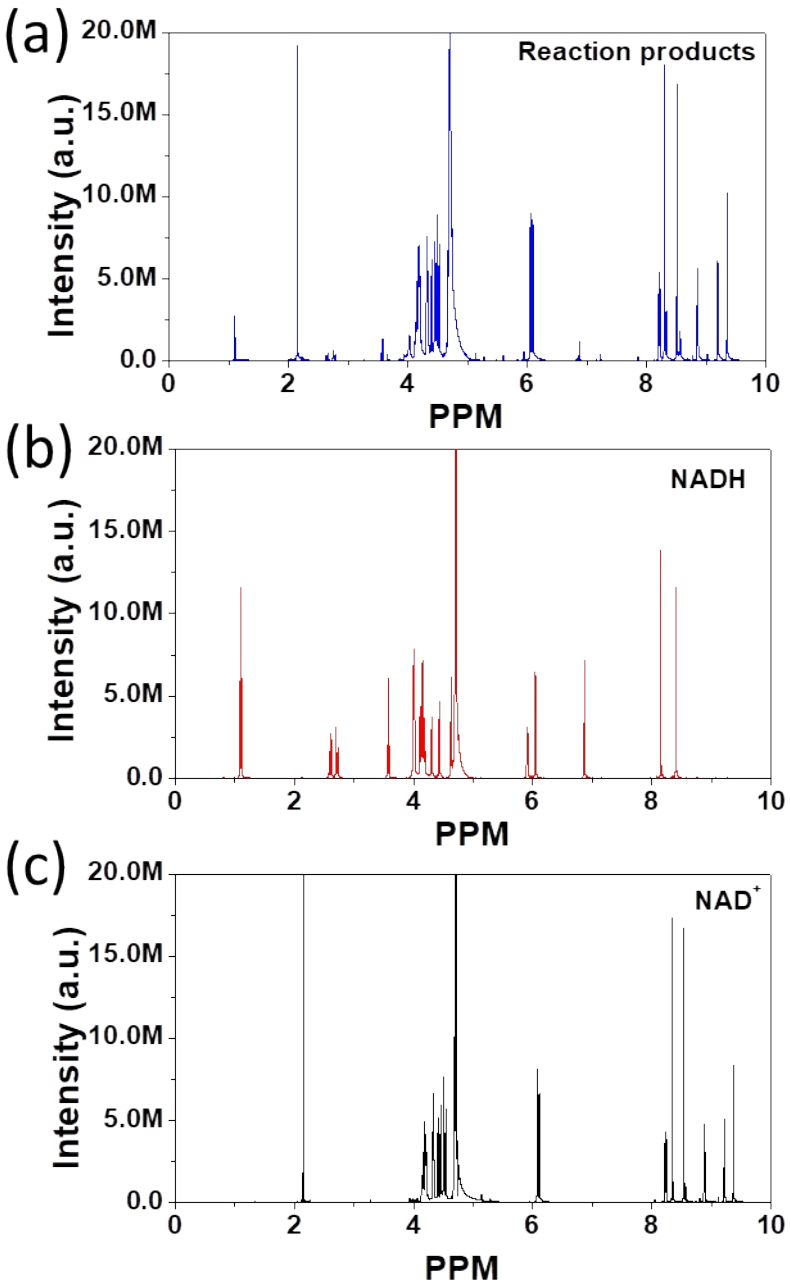

Figure S7. The ^{1}H NMR spectra of NAD^{+}, NADH and the reaction products after AM/M/BP HNPs catalyzed under light irradiation.

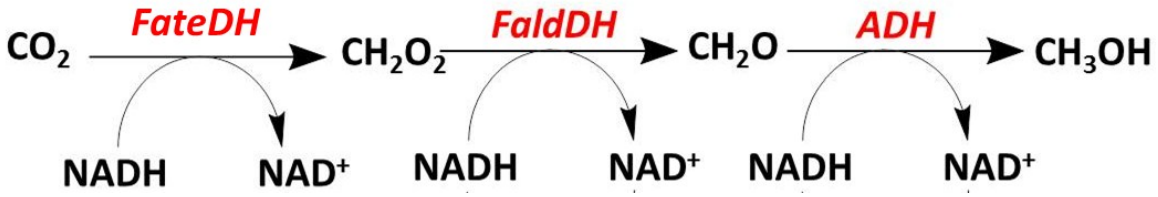

Figure S8. Schematic illustration of the conversion of methanol from CO_2 by FateDH, FaldDH, and ADH mediated cascade reaction.

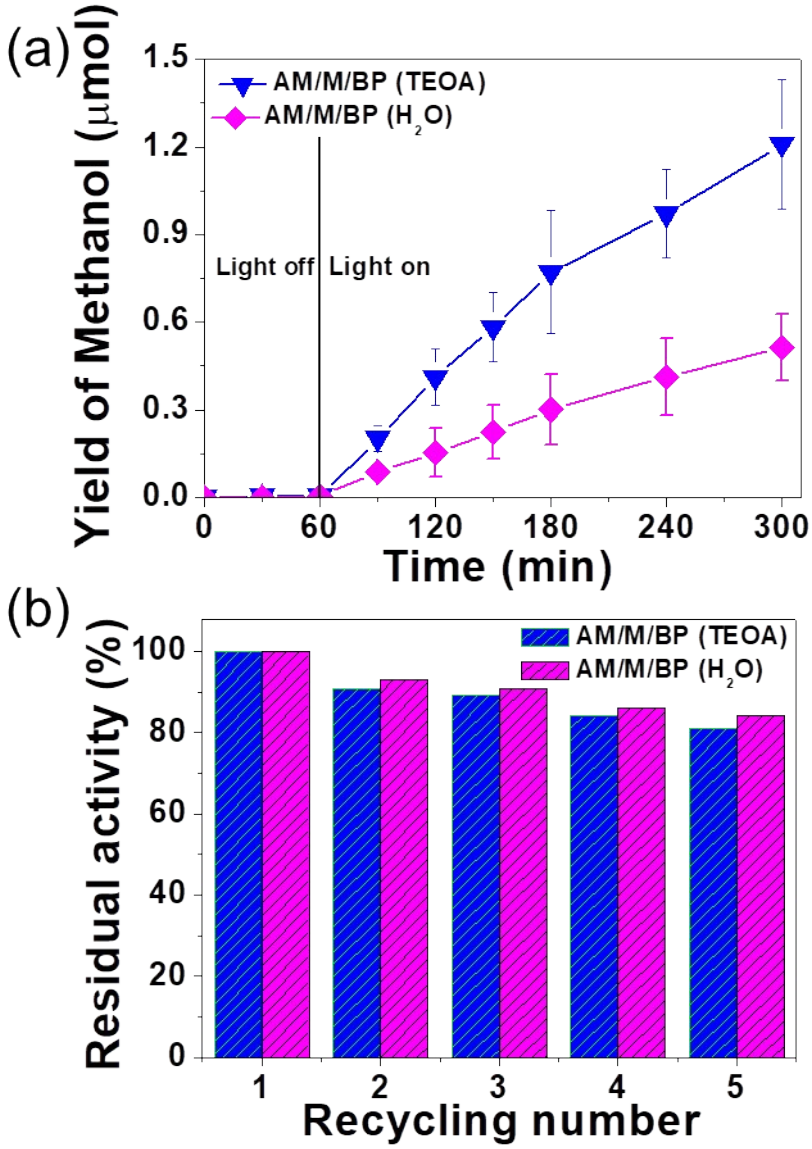

Figure S9. (a) The synthesis of methanol from CO_2 as a function of reaction time catalyzed by this cascade reaction with photocatalyzed NADH regeneration using TEOA or H_2O as electron donor. (b) The stability of reaction of (a).

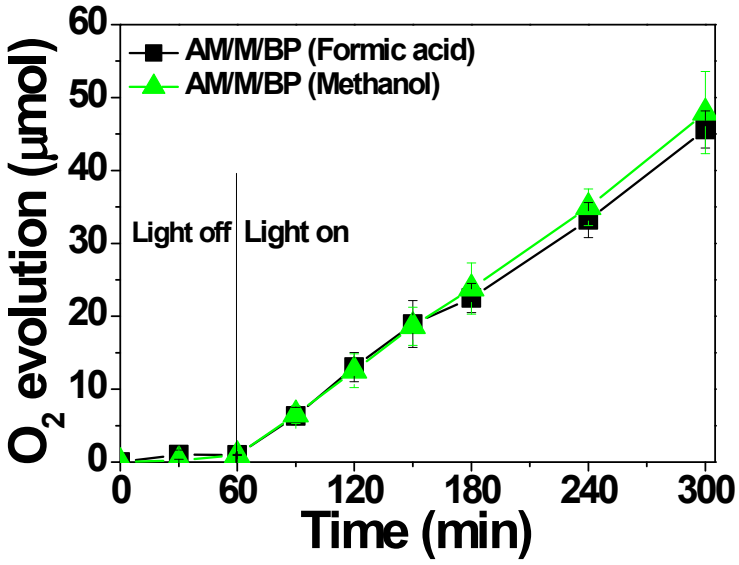

Figure S10. The O_2 evolution curves of AM/M/BP HNSs based APS catalyzing formic acid conversion from CO_2, L-glutamate from α-ketoglutarate, and methanol conversion from CO_2.

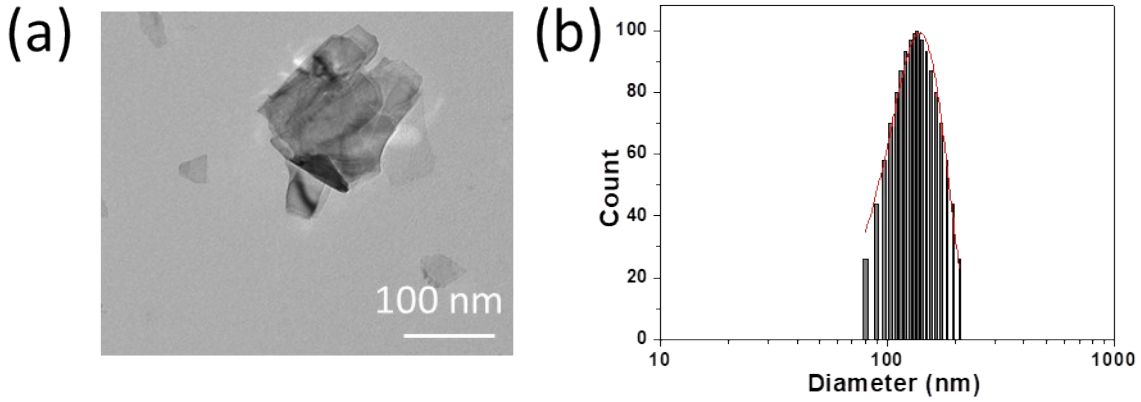

Figure S11. (a) TEM images and (b) size distribution of AM/M/BP NSs after 5 cycles of reuse.

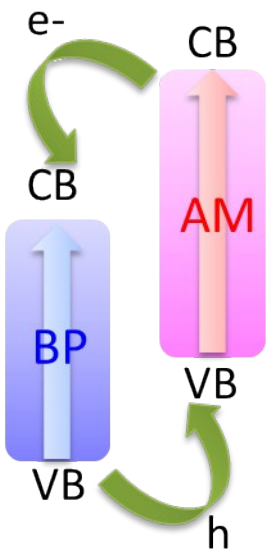

Figure S12. Potential type II heterojunction electron transfer pathway in AM/BP HNSs.

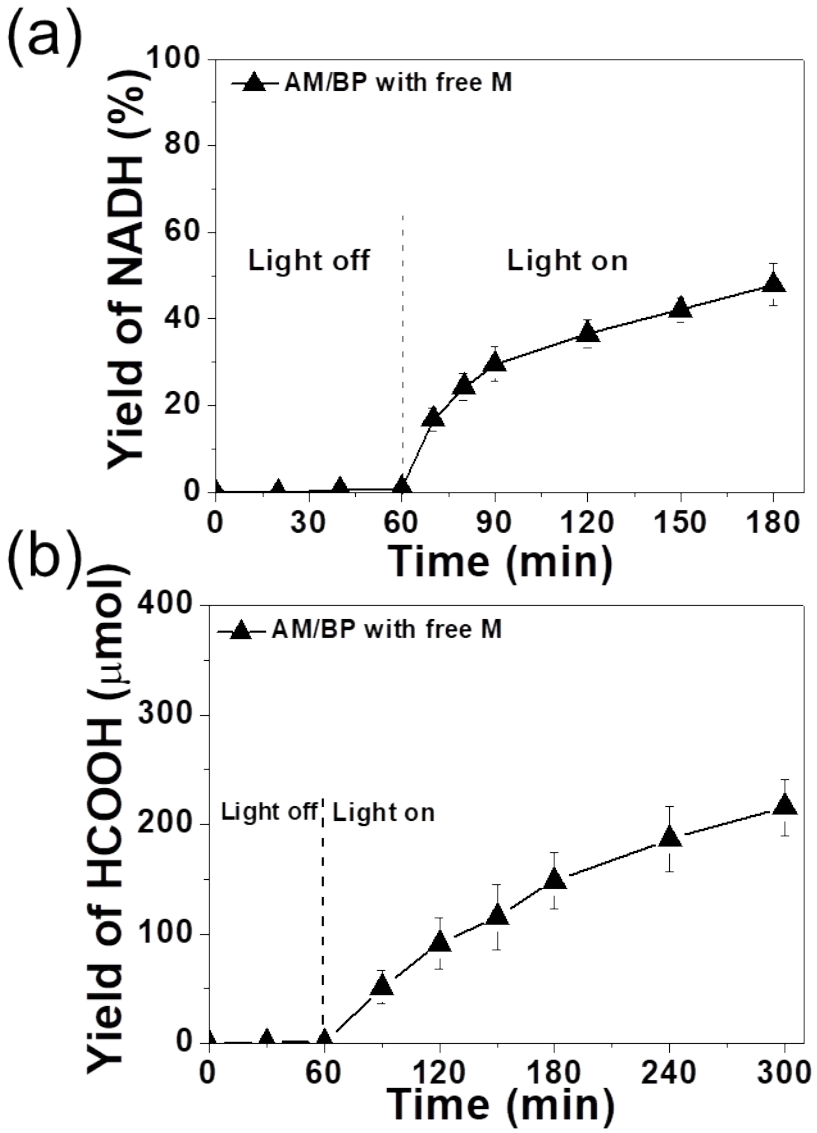

Figure S13. (a) Time profiles of the photocatalytic regeneration of NADH from NAD^+, (b) time profiles of the CO_2 conversion to formic acid of AM/BP HNSs with free M.

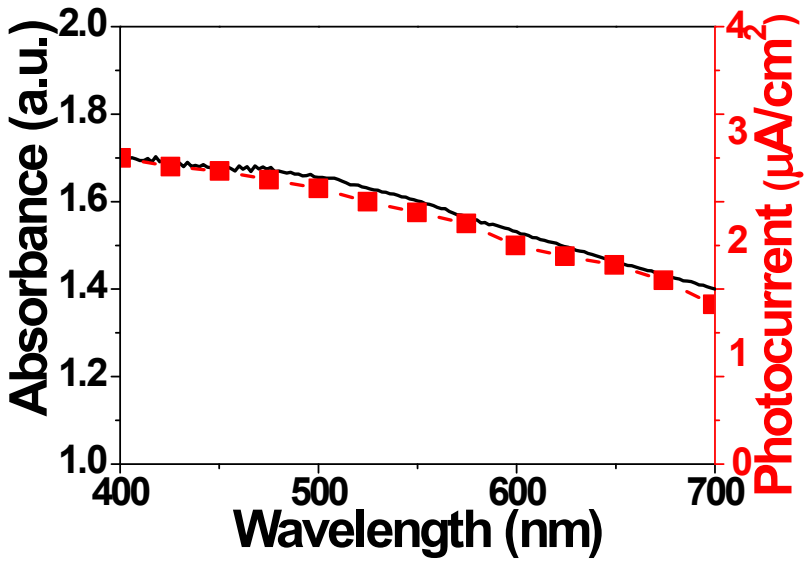

Figure S14. Visible absorbance and photocurrent action spectra of AM/M/BP HNSs.

Table S1. The final amount and activity recovery of each component on AM/M/BP HNSs.

	M	FDH	NAD^+
Amount	0.51 μmol/mg-HNSs	1.4 unit/mg-HNSs	0.49 μmol/mg-HNSs
Activity recovery	97.56%	83.14%	94.86%

Table S2. Comparison of the artificial photosynthesis efficacy obtained in the present work with values reported by others.

Photocatalyst		Electron donor	Electron mediator	NADH yield (%)[a]	TOF (h^{-1})[b]	QE (%)[c]	Enzyme	TON (NADH)/ h^{-1} [d]	TON (E)/h^{-1} [e]	Ref
Organic dyes	Eosin Y	TEOA (15%)	M_{bpy} (0.25 mM)	48		3.5	GDH	5	10×10^3	[4]
	Zn-containing porphyrin	TEOA (15%)	M_{bpy} (0.25 mM)	20	0.5					[5]
	Proflavine	TEOA (15%)	M_{bpy} (0.25 mM)	63			GDH	33		[6]
	TP-COF	TEOA (15%)	M_{bpy} (0.25 mM)	90			GDH	2		[7]
	Triptycene-based 3D Polymer Film	TEOA (15%)	M_{bpy} (0.25 mM)	50			FateDH	54	5×10^4	[8]
Inorganic semiconductors	Hydrogen-Terminated Silicon Nanowires	TEOA (15%)	M_{bpy} (0.25 mM)	65			GDH	0.4	1×10^3	[9]
	Upconversion nanoparticles	TEOA (15%)	M_{bpy} (0.25 mM)	19			GDH	2	1×10^3	[10]
	CdS QDs	TEOA (15%)	M_{bpy} (0.25 mM)	54	0.12					[11]
	CdSe QDs	TEOA (15%)	M_{bpy} (0.25 mM)	30	0.17					
	CdTe QDs	TEOA (15%)	M_{bpy} (0.25 mM)	54	0.54					
	$W_2Fe_4Ta_2O_{17}$	EDTA (5 mM)	M_{bpy} (0.25 mM)	10	0.002		GDH	0.006	13	[12]
		H_2O	M_{bpy} (0.25 mM)	5						

	$[Co_4(H_2O)_2(PW_9O_{34})_2]^{10-}$	H_2O	$M_{4\text{-dcbpy}}$ (1 mM)	<10			GDH	0.2	465	[13]
	TaS_2 NSs	TEOA (15%)	M_{phen}(0.25 mM)	50		7	FateDH	13	4×10^3	[14]
Hybrid nanomaterials	Porphyrin synthetic wood film	TEOA (15%)	M_{bpy} (0.25 mM)	45			GDH	0.3	228	[15]
	CdS QDs-sensitized SiO_2 nanoparticles	TEOA (15%)	M_{bpy} (0.25 mM)	65			GDH	0.6	3×10^3	[16]
	CdS QDs-sensitized TiO_2 nanotubes	TEOA (15%)	M_{bpy} (0.25 mM)	35			GDH	0.6	2×10^3	[17]
	nPt-sensitized porphyrin–peptide nanotubes	TEOA (15%)	M_{bpy} (0.5 mM)	18	1.78		GDH	1.5	5×10^3	[18]
	Graphene with attached isatin–porphyrin	TEOA (15%)	M_{bpy} (0.2 mM)	39			FateDH/ FaldDH/ ADH	8×10^{-5}	10	[19]
	PDA-Au-EY nanohybrid films	TEOA (15%)	M_{bpy} (0.5 mM)	13			GDH	0.3	1×10^3	[20]
	Porphyrin/SiO_2/Cp* Rh(bpy)Cl Hybrid Nanoparticles	TEOA (15%)	M_{bpy} (0.15 mM)	40		13	FateDH	25	8×10^3	[21]
	Graphene-based photocatalyst (CCGCMAQSP)	TEOA (15%)	M_{bpy} (0.2 mM)	30		9	GDH	45	2×10^4	[22]
	Graphene–BODIPY	TEOA (15%)	M_{bpy} (0.2 mM)	33		10	GDH	58	2×10^4	[23]
	g-C_3N_4@α-Fe_2O_3/C Core@Shell Photocatalysts	TEOA (15%)	M_{bpy} (0.2 mM)	76		17	FaldDH/ ADH	2	3×10^3	[24]
	Graphene oxide modified with cobalt metallated aminoporphyrin	TEOA (15%)	MV^{2+} (2 mM),	30			FateDH	52	2×10^4	[25]

Integrated system	TaS2–PEG–GR–M	TEOA (15%)	M_{phen}(0.25 mM)	80		15.03	FateDH	20	7×10^3	[14]
	AM/M/BP HNSs	TEOA (15%)	M_{phen}(0.1 mM)	79±0.7	0.5±0.1	18±0.4	FateDH	91±0.3	$(3\pm0.1)\times10^4$	
							FateDH/ FaldDH/ ADH	0.9±0.1	133±1.2	
		H_2O		30±0.6	0.2±0.1	6±0.1	FateDH	40±0.5	$(1\pm0.4)\times10^4$	
							FateDH/ FaldDH/ ADH	0.2±0.04	24±0.5	

[a] NADH regeneration yields after 1 h irradiation of visible light were compared.

[b] Turnover Frequency (TOF) is the total number of moles transformed into the desired product by one mole of catalyst per hour.

[c] Quantum Efficiency (QE) is the ratio of the number of charge carriers collected to the number of photons of a given energy.

[d] Turnover Number (TON) of NADH is the total number of moles transformed into the desired product by one mole of NADH per hour.

[e] Turnover Number (TON) of enzyme is the total number of moles transformed into the desired product by one mole of enzyme per hour.

References

[1] C. Gibaja, D. Rodriguez-San-Miguel, P. Ares, J. Gomez-Herrero, M. Varela, R. Gillen, J. Maultzsch, F. Hauke, A. Hirsch, G. Abellan, F. Zamora, *Angew. Chem. Int. Ed. Engl.* 2016, *55*, 14345.

[2] W. Tao, X. Zhu, X. Yu, X. Zeng, Q. Xiao, X. Zhang, X. Ji, X. Wang, J. Shi, H. Zhang, L. Mei, *Adv. Mater.* 2017, *29,* 1603276.

[3] a) X. Ji, Y. Kang, Z. Su, P. Wang, G. Ma, S. Zhang, *ACS Sustain. Chem. Eng.* 2018, *6*, 3060; b) X. Ji, C. Liu, J. Wang, Z. Su, G. Ma, S. Zhang, *J. Mater. Chem. A* 2017, *5*, 5511; c) X. Ji, J. Wang, Y. Kang, L. Mei, Z. Su, S. Wang, G. Ma, J. Shi, S. Zhang, *ACS Catal.* 2018, *8*, 10732.

[4] S. H. Lee, H. J. Lee, K. Won, C. B. Park, *Chem. Eur. J.* 2012, *18*, 5490.

[5] J. H. Kim, S. H. Lee, J. S. Lee, M. Lee, C. B. Park, *Chem. Commun.* 2011, *47*, 10227.

[6] D. H. Nam, C. B. Park, Chembiochem 2012, *13*, 1278.

[7] Y. Zhao, H. Liu, C. Wu, Z. Zhang, Q. Pan, F. Hu, R. Wang, P. Li, X. Huang, Z. Li, *Angew. Chem. Int. Ed.* 2019, *58*, 5376.

[8] R. K. Yadav, A. Kumar, D. Yadav, N. J. Park, J. Y. Kim, J. O. Baeg, *Chemcatchem* 2018, *10*, 2024.

[9] H. Y. Lee, J. Ryu, J. H. Kim, S. H. Lee, C. B. Park, *Chemsuschem* 2012, *5*, 2129.

[10] J. S. Lee, D. H. Nam, S. K. Kuk, C. B. Park, *Chem. Eur. J.* 2014, *20*, 3584.

[11] D. H. Nam, S. H. Lee, C. B. Park, *Small* 2010, *6*, 922.

[12] C. B. Park, S. H. Lee, E. Subramanian, B. B. Kale, S. M. Lee, J. O. Baeg, *Chem. Commun.* 2008, *42*, 5423.

[13] R. Jungki, N. D. Heon, L. Sahng Ha, P. C. Beum, *Chem. Eur. J.* 2014, *20*, 12020.

[14] X. Ji, C. Liu, J. Wang, Z. Su, G. Ma, S. Zhang, *J. Mater. Chem. A* 2017, **5**, 5511.

[15] M. Lee, J. H. Kim, S. H. Lee, S. H. Lee, C. B. Park, *Chemsuschem* 2011, *4*, 581.

[16] S. H. Lee, J. Ryu, D. H. Nam, C. B. Park, *Chem. Commun.* 2011, *47*, 4643.

[17] J. Ryu, S. H. Lee, D. H. Nam, C. B. Park, *Adv. Mater.* 2011, *23*, 1883.

[18] J. H. Kim, M. Lee, J. S. Lee, C. B. Park, *Angew. Chem. Int. Ed.* 2012, *51*, 517.

[19] R. K. Yadav, G. H. Oh, N.-J. Park, A. Kumar, K.-j. Kong, J.-O. Baeg, *J. Am. Chem. Soc.* 2014, *136*, 16728.

[20] M. Lee, J. U. Kim, J. S. Lee, B. I. Lee, J. Shin, C. B. Park, *Adv. Mater.* 2014, *26*, 4463.

[21] X. Ji, J. Wang, L. Mei, W. Tao, A. Barrett, Z. Su, S. Wang, G. Ma, J. Shi, S. Zhang, *Adv. Funct. Mater.* 2018, *28,* 1705083.

[22] R. K. Yadav, J.-O. Baeg, G. H. Oh, N.-J. Park, K.-j. Kong, J. Kim, D. W. Hwang, S. K. Biswas, *J. Am. Chem. Soc.* 2012, *134*, 11455.

[23] R. K. Yadav, J.-O. Baeg, A. Kumar, K.-j. Kong, G. H. Oh, N.-J. Park, *J. Mater. Chem. A* 2014, *2*, 5068.

[24] Y. Wu, J. Ward-Bond, D. Li, S. Zhang, J. Shi, Z. Jiang, *ACS Catal.* 2018, *8*, 5664.

[25] S. Kumar, R. K. Yadav, K. Ram, A. Aguiar, J. Koh, A. J. F. N. Sobral, *J. CO_2 Util.* 2018, *27*, 107.